Massive point-vortex simulation using special-purpose computer, MDGRAPE-3 (Fast Algorithms in Computational Fluids : theory and applications)

AUTHOR(S):

YATSUYANAGI, Yuichi

数理解析研究所講究録
第1606巻 2008年 1-17

Massive point-vortex simulation using special-purpose computer, MDGRAPE-3

YATSUYANAGI, Yuichi *
Faculty of Education, Shizuoka University

1 Introduction

Our final goal is to understand characteristics of negative temperature state appearing in dynamics of two-dimensional point vortex system [1].

We began a simulation of the point vortex system to understand results of nonneutral plasma experiments obtained by Kiwamoto group at Kyoto University. It can be shown that the electron motion in the plane perpendicular to the strong, uniform magnetic field is given by two-dimensional Euler equation. In the same sense, the governing equation for the two-dimensional guiding-center plasma that is a collection of charged rods is identical to that of two-dimensional, inviscid, incompressible fluid.

One of the most remarkable features of the point vortex system is the negative temperature state first introduced by Onsager [2]. Two-dimensional point vortex system confined in a finite area has limited phase space volume, so that in the limit of infinite system energy, the density of state approaches zero and has at least one peak at some energy E_0. Following the statistical definition of temperature, $1/T = dS/dE = k_B d\ln W/dE$, where T is temperature, S is entropy, E is energy, k_B is Boltzmann constant, and W is density of state, the sign of temperature changes if system energy is larger than E_0. Note that there is no concept of negative absolute temperature in the thermodynamic sense. However, as is mentioned by Onsager, there are many phenomena that can be well-described by assuming negative statistical temperature, even if the thermodynamic temperature is positive [2]. We consider that characteristic features that originate in the negative temperature may appear in the dynamics of the point vortex system.

Wide variety of research effort has been devoted to understand the negative temperature state in the context of two-dimensional turbulence. The condensation of the same-sign vortices in the rectangular domain is first demonstrated numerically by Joyce

*eyyatsu@ipc.shizuoka.ac.jp

and Montgomery [3]. The equilibrium state in the negative temperature is discussed by Pointin and Lundgren [4]. The density of states is obtained by analytically by Seyler [5] and numerically by Buehler [6] and Johnson [7]. However, these simulation results are very restricted ones in the number of particles and resolution due to the limited calculation power. Thus, we started the point vortex simulation on the negative temperature state using recent high performance computers.

In the point vortex simulation, time evolution of the point vortices is traced by the vorticity equation. To update the position of the point vortex, the flow velocity at each point vortex must be calculated. This calculation is called the Biot-Savart integral, and its calculation cost is proportional to the square number of the total point vortices. There are some different solutions for reducing the calculation cost:

- Use a fast algorithm.
- Use a PC cluster.
- Use a supercomputer.

For PC-based simulations, the most practical solution may be to use a fast algorithm, for example, tree code and Vortex-In-Cell approximation. However, the integral precision is also usually reduced. For our case, this is a severe problem as the target system in negative temperature is high energy one and to trace the trajectory of the motion of vortices, the velocity at each point vortex should be evaluated exactly at the position of the point vortex.

The second candidate, PC cluster, has become a very popular solution for massive simulations. Even a university laboratory can bear the cost and the space to maintain a small cluster. However, in our case, total calculation speed necessary is approximately 100 GFlops over and more than 50 PCs are required to achieve this speed. So, we decided to choose the third solution, using a supercomputer called MDGRAPE series. It was originally designed for molecular dynamics simulation. By using a capability of arbitrary choice of Green's function, Biot-Savart integral also can be calculated by it. It provides 350 GFlops calculation speed. This means approximately 100 times faster than a usual PC.

By the massive simulations using MDGRAPE series, two-dimensional point vortex system is examined and characterized by temperature. At first, we examine the density of states if it has a peak. Equilibrium distributions are obtained by time asymptotically. We find that slope of the energy spectrum in the intermediate wave number depends on the system energy. Two-body correlation function is used for detailed analysis for the equilibrium distribution.

The organization of this paper is as follows. In §2, the prelude of this research is reviewed. In §3, the negative temperature state in the point-vortex system is reviewed.

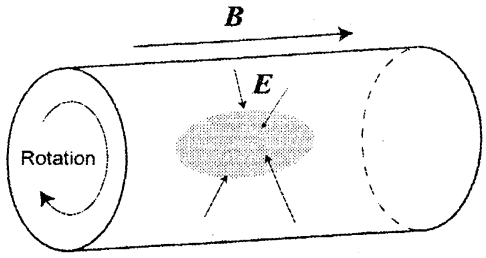

Figure 1: Schematic of confinement geometry is shown. Strong axial magnetic field and edge electrostatic potential confines electrons. They rotate in $\boldsymbol{E} \times \boldsymbol{B}$ direction.

In §4, special-purpose supercomputer, MDGRAPE-2 and -3 are introduced. In §5, we show simulation results on the point vortex system characterized by the temperature.

2 Prelude of this research: Nonneutral plasma experiment

We started numerical simulations of the point vortex system to understand the results of nonneutral plasma experiments carried out by Kiwamoto group at Kyoto University.

Electrons are confined in a circular cylinder axially by an electrostatic potential and radially by a strong uniform magnetic field. Schematic configuration of confinement is shown in Fig. 1. Typical time scales of the electron motion satisfy

$$\tau_c \ll \tau_{E\times B} \ll \tau_{\text{bounce}}, \tag{1}$$

where τ_c denotes a period for an electron cyclotron motion, $\tau_{E\times B}$ is a time scale for $\boldsymbol{E} \times \boldsymbol{B}$ motion, and τ_{bounce} is a time scale for an electron to bounce between the ends by the electrostatic potential. As long as the radius of the cyclotron motion is small enough, the electron motion can be represented by the motion of the guiding center. In this limit, the equation of the electron motion in the two-dimensional plane perpendicular to the magnetic field is identical to the Euler equation for inviscid, incompressible fluid.

Let the direction of the strong magnetic field be z,

$$\boldsymbol{B} = B_0 \hat{\boldsymbol{z}}. \tag{2}$$

Equation of motion of the guiding center is given by

$$m_e \frac{d\boldsymbol{v}}{dt} = -e(\boldsymbol{E} + \boldsymbol{v} \times \boldsymbol{B}). \tag{3}$$

By time averaging Eq. (3) over a cycle, the drift velocity of the guiding center is given by the usual $\boldsymbol{E} \times \boldsymbol{B}$ drift

$$\boldsymbol{v} = \frac{\boldsymbol{E} \times \boldsymbol{B}}{|\boldsymbol{B}|^2}. \tag{4}$$

Incorporating electrostatic potential induced by the electrons themselves

$$\boldsymbol{E} = -\nabla\phi \tag{5}$$

and Eq. (2) into Eq. (4), we obtain

$$\boldsymbol{v} = \frac{1}{B_0}\hat{\boldsymbol{z}} \times \nabla\phi. \tag{6}$$

Thus, the self electrostatic potential behaves like a stream function for a two-dimensional flow. Rotation of Eq. (6) gives the vorticity

$$\omega_z\hat{\boldsymbol{z}} = \nabla \times \boldsymbol{v} = \frac{\hat{\boldsymbol{z}}}{B_0}\nabla^2\phi = \frac{en}{\epsilon_0 B_0}\hat{\boldsymbol{z}}, \tag{7}$$

where n is the number density of the electron. In the last term, Poisson equation is used

$$\nabla^2\phi = \frac{en}{\epsilon_0}. \tag{8}$$

Equation (7) tells that the vorticity is proportional to the number density of the electron. By these relations, the governing equation of guiding-center plasma is found to be identical to the Euler equation. More complete description for the electron confinement is available in Ref. [8].

3 Negative temperature state appearing in two dimensional point vortex system

Large-scale, long-lived vortices are commonly observed in nearly two-dimensional flow. It can also be seen in the nonneutral plasma experiment. Initially doughnut-shaped electron distribution is deformed into several clumps by the diocotron instability, or more famous words, Kelvin-Helmholtz instability. The number of clumps produced initially is understood by the linear theory [9]. Shortly, merger continuously occurs and the number of clumps gradually decreases in time. In this process, each clump size increases, which indicates the energy transfer from a short scale to a large scale, i.e., the inverse energy cascade.

For decades, various investigations have been made to understand the inverse energy cascade [10, 11]. Onsager introduced a concept of "negative temperature" for the two-dimensional point vortex system in 1949 to understand the large-scale vortex formation [2]. When temperature T is positive, vortices of opposite sign will tend to approach each other. On the other hand, when T is negative, vortices of the same sign will tend to cluster and preferably form stronger vortex. This statistical tendency of the same sign to cluster in the negative temperature region is clear from a description by a canonical

energy distribution proportional to $\exp(-\beta E)$. Negative β corresponds to reversing the sign of the interaction, where the same-sign vortices statistically attract and opposite ones repel [12].

Here we explain a target point vortex system, including the basic concept of negative temperature. We consider a point vortex system consisting of N positive and N negative point vortices with circulation $\Gamma_0 = \text{const.}$ and $-\Gamma_0$, respectively, bounded by a circular wall of radius R. Position vector and circulation of the i-th point vortex is given by $\boldsymbol{r}_i$ and Γ_i, respectively. Constants of motion are Hamiltonian and inertia:

$$H = -\frac{1}{4\pi}\sum_{i}^{N}\sum_{j\neq i}^{N}\Gamma_i\Gamma_j \ln|\boldsymbol{r}_i - \boldsymbol{r}_j| + \frac{1}{4\pi}\sum_{i}^{N}\sum_{j}^{N}\Gamma_i\Gamma_j \ln|\boldsymbol{r}_i - \bar{\boldsymbol{r}}_j| - \frac{1}{4\pi}\sum_{i}^{N}\sum_{j}^{N}\Gamma_i\Gamma_j \ln\frac{R}{|\boldsymbol{r}_j|} \tag{9}$$

$$I = \sum_{i}^{N}\Gamma_i|\boldsymbol{r}_i|^2 \tag{10}$$

The last term in Eq. (9) is introduced to make the value of stream function at the circular wall zero. Equations of motion for each point vortex are given by

$$\Gamma_i\frac{dx_i}{dt} = \frac{\partial H}{\partial y_i}, \quad \Gamma_i\frac{dy_i}{dt} = -\frac{\partial H}{\partial x_i}, \tag{11}$$

or explicitly

$$\frac{d\boldsymbol{r}_i}{dt} = -\frac{1}{2\pi}\sum_{j\neq i}^{2N}\Gamma_j\frac{(\boldsymbol{r}_i - \boldsymbol{r}_j)\times\hat{\boldsymbol{z}}}{|\boldsymbol{r}_i - \boldsymbol{r}_j|^2} + \frac{1}{2\pi}\sum_{j}^{2N}\Gamma_j\frac{(\boldsymbol{r}_i - \bar{\boldsymbol{r}}_j)\times\hat{\boldsymbol{z}}}{|\boldsymbol{r}_i - \bar{\boldsymbol{r}}_j|^2}. \tag{12}$$

The wall effect is introduced by the image vortex located at $\bar{\boldsymbol{r}}_i = R^2\boldsymbol{r}_i/|\boldsymbol{r}_i|^2$.

The inverse temperature β is statistically defined by

$$\beta = \frac{dS}{dE} = k_B\frac{d\ln W(E)}{dE}. \tag{13}$$

In usual cases, $W(E)$ increases as E increases, and the slope dS/dE never changes the sign, i.e., always positive (Fig. 2). On the other hand, if the total phase space volume is finite, the total number of states is limited, and the asymptotic value of the density of state at infinite energy must be zero. Then the density of state should have at least a peak at some energy E_0. So that, in the region of $E > E_0$, temperature is negative.

Onsager considered that the x_i and y_i coordinates of each point vortex are canonical conjugates due to the similarity of the equations of motion of the point vortices (11) to the common Hamilton equation. Namely, the phase space of the point vortex system is identical to the configuration space. Assuming that the vortices are confined in an area A, total phase space volume is given by

$$\int d\Omega = \int dx_1dy_1\cdots dx_{2N}dy_{2N} = \left(\int dxdy\right)^{2N} = A^{2N}. \tag{14}$$

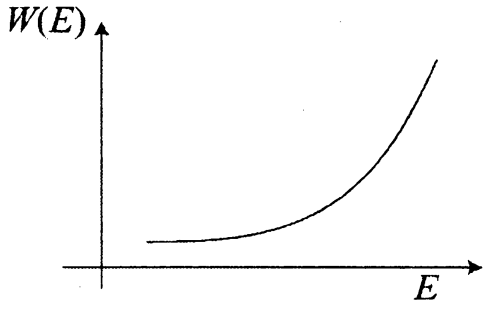

Figure 2: Usual relation between the density of state and the system energy is shown.

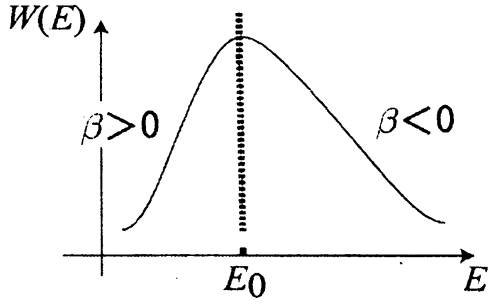

Figure 3: The density of state has at least a peak when the total number of states is limited. In this case, negative temperature state appears when $E > E_0$.

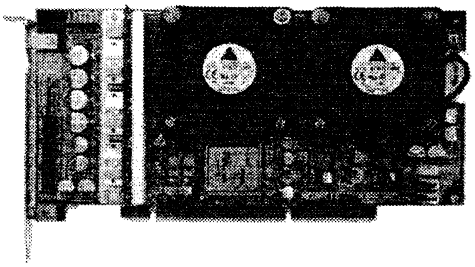

Figure 4: MDGRAPE-3 is a PCI-X card.

Thus, Onsager concluded that the negative temperature state appears in the two-dimensional point vortex system confined in a finite area. Since then, many simulation results have been presented to understand the two-dimensional point vortex system in statistical mechanical framework. However, numerical simulation on point vortex system demands relatively large calculation power. We noticed that there were few large scale simulation on the point vortex system in negative temperature state, so that we decided to investigate it by on-hand supercomputer, MDGRAPE-2 and MDGRAPE-3.

4 An accelerator for vortex simulations, MDGRAPE-3

To speed up the calculation in central processing unit (CPU), it is very efficient to restrict the types of calculation and completely implement them as a wired-logic device [13]. An extreme example is a special-purpose computer that can calculate usually only one kind of calculation. One of the most famous special-purpose computers may be GRAPE hardware that was at first developed at University of Tokyo [14]. The type of calculation is limited to the gravitational force for n stars. So that, GRAPE can be regarded as a fast Poisson solver for a three-dimensional system. As a branch of GRAPE, MDGRAPE series was developed. It has a capability to integrate Poisson equation with different Green function from the three-dimensional one, for example, Van der Waals force, two-dimensional Coulomb force, Biot-Savart integral.

Calculation time for each time step is measured in the point vortex simulation with time development by 4th order Runge-Kutta method. The simulations are executed as (a) a single thread on dual core CPU, (b) two threads on dual core CPU, (c) four threads on quad core CPU, (d) a single thread with MDGRAPE-2 and (e) a single thread with MDGRAPE-3. For the two cases using MDGRAPE hardware, the Biot-Savart integral is accelerated by them. The result is shown in Fig. 5. Detailed specifications of the hardware used here are shown in Table 1. For 8036 point vortices case, calculation time

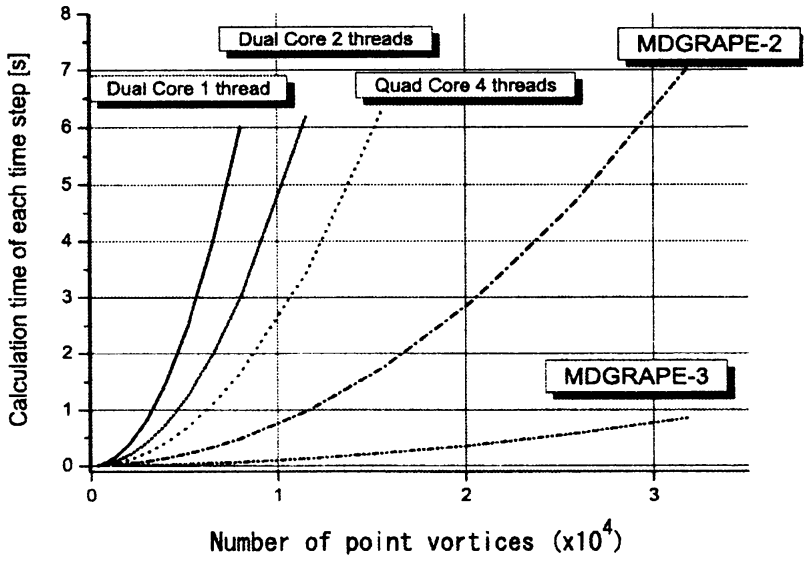

Figure 5: Calculation time per one time step is plotted against the number of point vortices without image vortices.

Table 1: Specifications of CPUs and memories.

Label	CPU	Memory	FSB Clock
Dual Core	Core 2 Duo E6750 (2.66GHz)	DDR2 800 4GB	1333MHz
Quad Core	Core 2 Quad Q6600 (2.4GHz)	DDR2 800 4GB	1066MHz
MDGRAPE-2	Pentium4 2.4GHz	DDR 266 512MB	533MHz
MDGRAPE-3	Pentium4 660 (3.6GHz)	DDR2 667 2GB	800MHz

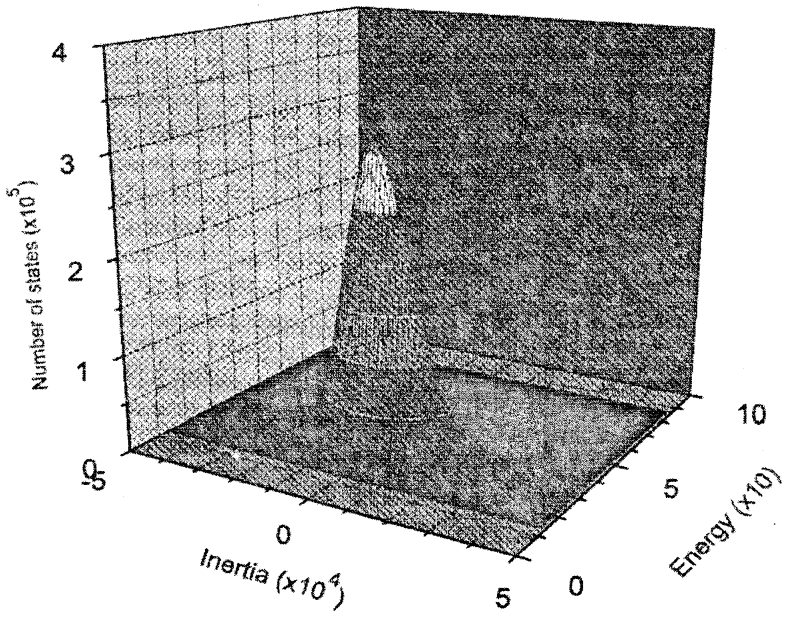

Figure 6: Density of state is plotted against system energy E and inertia I.

is (a) 6.01 sec., (b) 3.01 sec., (c) 1.67 sec., (d) 0.49 sec., (e) 0.068 sec.. The speed ratio to (a) is (a) 1.00, (b) 1.99, (c) 3.59, (d) 12.2, (e) 88.5. In other words, MDGRAPE-3 finishes simulation for a day that takes 89 days with PC without MDGRAPE-3.

5 Characterization of point vortex system by temperature

In this section, we demonstrate the simulation results for the statistical understanding of the two-dimensional point vortex system [1].

5.1 Density of state

To check the existence of the negative temperature state in the target point vortex system, the density of state is obtained by a random sampling of states following the micro canonical statistics. Each state is characterized by energy E and inertia I which are determined by randomly generated distribution of point vortices. Density of state consisting of 10^8 states is shown in Figs. 6 and 7. The density of state has a peak at $E = 29.1$ and $I = 0.0$, which gives an evidence for the negative temperature state. The ridge extends on $I = 0$ plane that is a symmetric plane of the density of state. As the

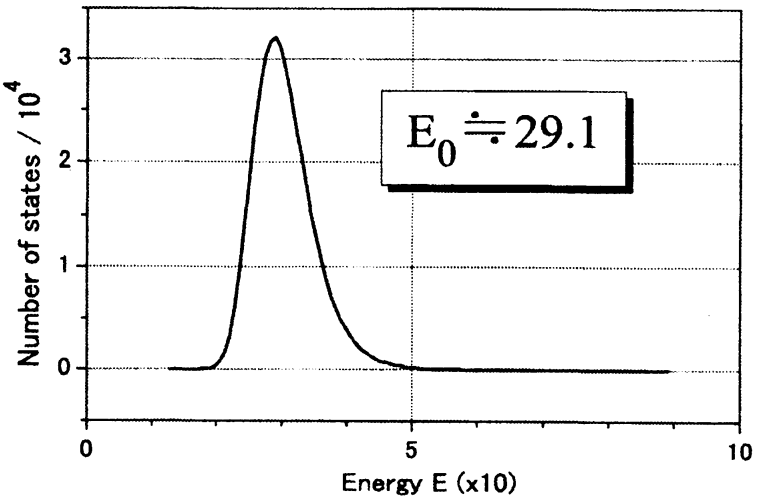

Figure 7: Density of state on $I = 0$ plane is shown.

number of vortices increases, the peak becomes steep one and peak position approaches $E = 0$.

5.2 Equilibrium distribution

It may be likely that equilibrium distribution of the vortices changes with the temperature. So, equilibrium distributions of the vortices at various values of temperature are obtained time-asymptotically by time development simulations. The temperature is controlled by the initial distribution of the vortices that determines the system energy. The results are shown in Fig. 8. In positive temperature, both sign of vortices mix with each other and spread over the circular area uniformly. On the other hand, when the sign of the temperature changes with energy increase, the same-sign vortices tend to form small clumps. In larger energy case, the clumps size becomes gradually large and the configuration finally reaches a dipole one. Note that the background vortices enable the clump formation that needs large energy in the energy conserving system. The energy belonging to the background vortices is relatively low compared with the vortices in the clumps.

5.3 Two-body correlation function

Here two-body correlation function is defined by a distribution of the distances for all combinations of two vortices. The value of the correlation function is normalized by

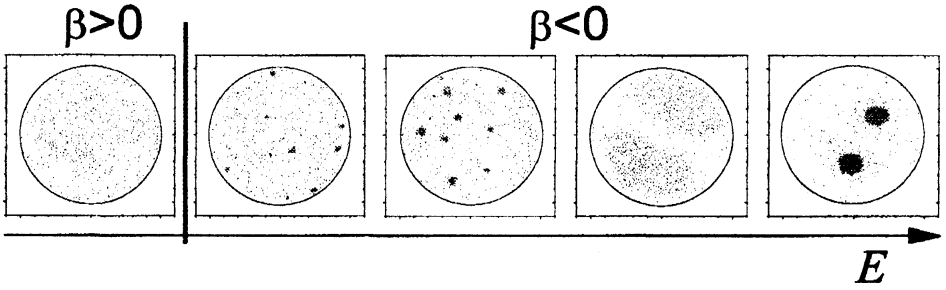

Figure 8: Equilibrium distributions of the vortices are shown. In the right edge distribution, the upper and lower clump exclusively consists of the positive and negative vortices, respectively.

the total number of the combinations of two vortices. In Fig. 9, the correlation function for the negative temperature case whose vortex distribution is given in the right edge in Fig. 8 is shown. In Fig. 10, the correlation function for the positive temperature case whose distribution is given in the left edge in Fig. 8 is shown. In each Fig., two lines are indicated. The first one corresponds the distance distribution of the positive vortices around the positive vortices, and the second one corresponds the distance distribution of the negative vortices around the positive vortices. The distance distribution of the negative vortices around the positive vortices and the one of the negative vortices around the negative vortices are omitted here, because the distributions of positive and negative vortices are symmetric in the circular area, and the omitted correlation functions are almost identical to the two cases indicated in Figs. 9 and 10. For the negative temperature case, the left peak corresponds the clump distribution of the same sign, and the right peak corresponds the clump distribution of the other sign. It clearly shows the clumping distribution.

In positive temperature case, two lines overlap with each other perfectly, so that we can see only a line. It means the distributions of the negative and positive vortices are uniform in the circular area.

5.4 Energy ($k-$)spectrum

Energy spectrum of the point vortex system bounded by a circular wall is obtained analytically by [15, 16],

$$
\begin{aligned}
E(k) &= \frac{1}{4\pi k}\sum_{i}^{N}\Gamma_i^2 + \frac{1}{4\pi k}\sum_{i}^{N}\sum_{j\neq i}^{N}\Gamma_i\Gamma_j J_0\left(k|\boldsymbol{r}_i-\boldsymbol{r}_j|\right) \\
&\quad -\frac{1}{2\pi k}\sum_{i}^{N}\sum_{j}^{N}\Gamma_i\Gamma_j\sum_{\ell=0}^{\infty}\epsilon_\ell\left(\frac{|\boldsymbol{r}_j|}{R}\right)^{\ell}\times J_\ell(kR)J_\ell(k|\boldsymbol{r}_i|)\cos\left(\ell(\varphi_i-\varphi_j)\right)
\end{aligned}
$$

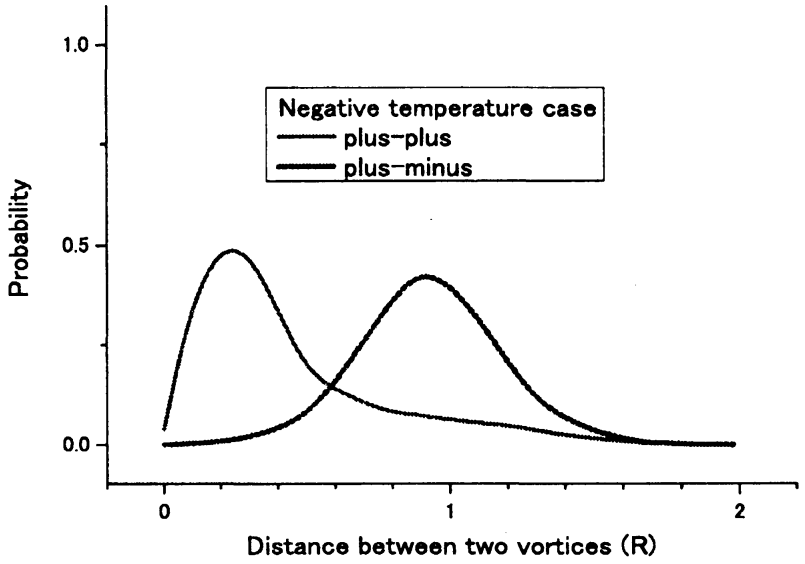

Figure 9: The correlation function for the negative temperature case whose vortex distribution is given in the right edge in Fig. 8 is shown..

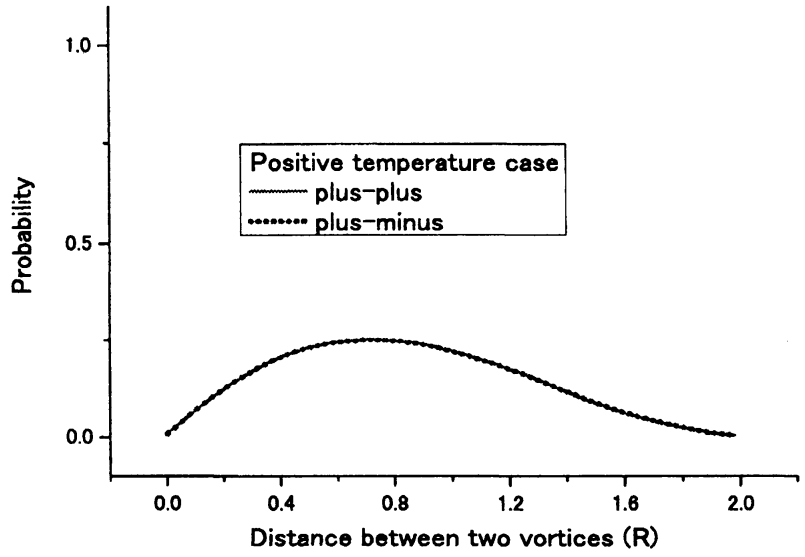

Figure 10: The correlation function for the positive temperature case whose distribution is given in the left edge in Fig. 8 is shown.

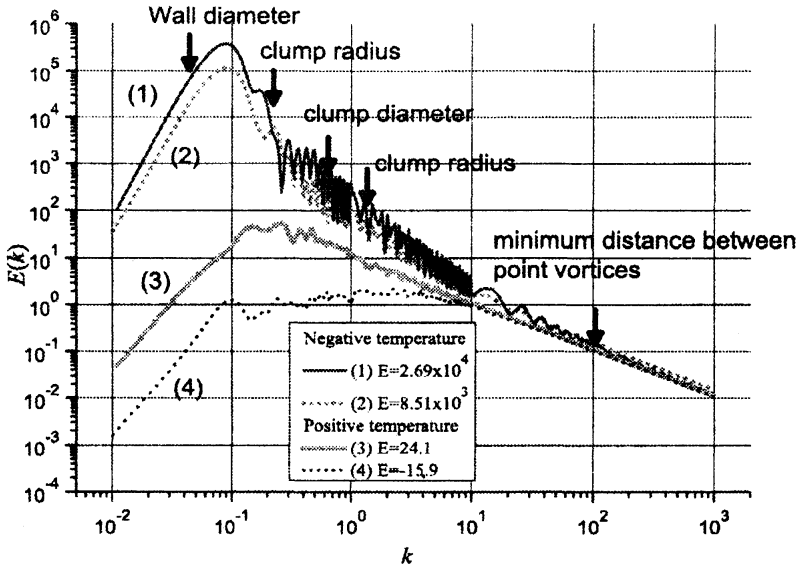

Figure 11: Energy spectra are plotted at various temperatures. The temperature is controlled by the initial configuration of the vortices.

$$+\frac{1}{2\pi k}\sum_{i}^{N}\sum_{j}^{N}\Gamma_i\Gamma_j\sum_{\ell=0}^{\infty}\epsilon_\ell\left(\frac{|\boldsymbol{r}_j|}{R}\right)^{\ell}\times J_\ell^2(kR)\cos\left(\ell(\varphi_i-\varphi_j)\right) \tag{15}$$

$$\epsilon_\ell = \begin{cases} 1 & \ell=0, \\ 2 & \ell\geq 1, \end{cases} \tag{16}$$

$$x_i = |\boldsymbol{r}_i|\cos(\varphi_i), \quad y_i = |\boldsymbol{r}_i|\sin(\varphi_i). \tag{17}$$

The first and the second terms obtained by Novikov gives the spectrum for unbounded point vortex system, and the rest represents the effect of the circular boundary. By using the formula (15), we obtain the spectra for various temperatures shown in Fig. 11. As is readily seen, the slope of the intermediate k decreases as the energy increases. Spectrum range is limited by the radius of the boundary in the small k region and by the minimum distance between the vortices in the large k region. In Fig. 12, the slope of the intermediate k is plotted against the system energy. Up to $E \approx 2\times 10^4$, the negative slope decreases with the energy increase. In larger energy, the slope approaches to a constant value, and the asymptotic value may be -2.0. However, it is possible that the slope cannot develop sharply due to a lack of simulation accuracy, i.e., integral precision is insufficient. Thus more detailed investigation is needed to conclude the slope approaches -2.0 in the high energy region.

In the positive temperature case, the slope should be -1 due to the cancellation of the terms in Eq. (15) by the uniform distribution of the positive and negative vortices.

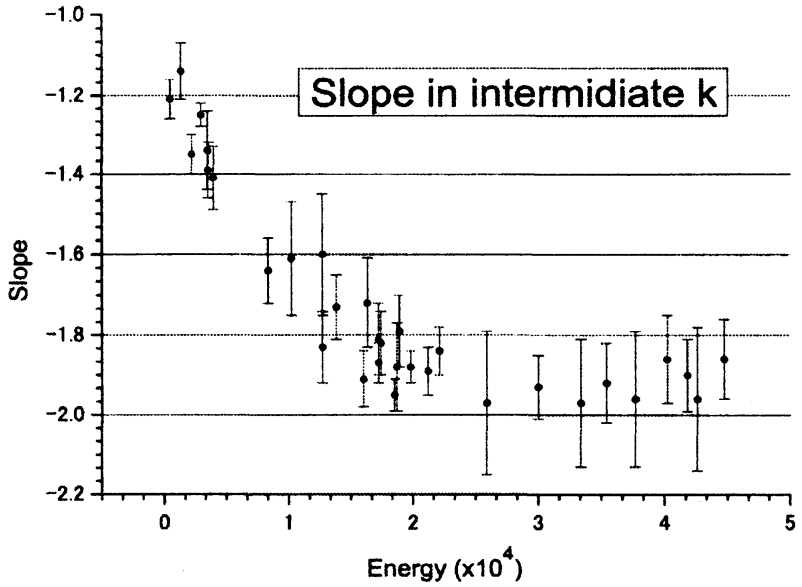

Figure 12: The slope in the intermediate k is plotted against the system energy.

However, there is a case where the slope is not -1 as shown in the lowest line in Fig. 11. Equilibrium distributions of the two cases where the slope is equal to -1 and unequal to -1 are shown in Fig. 13. One may understand that there is no remarkable difference between the two cases. However, the difference can be elucidated by the two body correlation function. The correlation functions are shown in Figs. 14 and 15 for the distributions in Fig. 13. The difference appears in the distribution probability of positive vortices around positive vortices. In Fig. 14 where the slope is equal to -1, the value approaches zero in the limit of zero distance. On the other hand, in Fig. 15, the value does not approach zero in the limit of zero distance. Thus the distribution probability of positive vortices

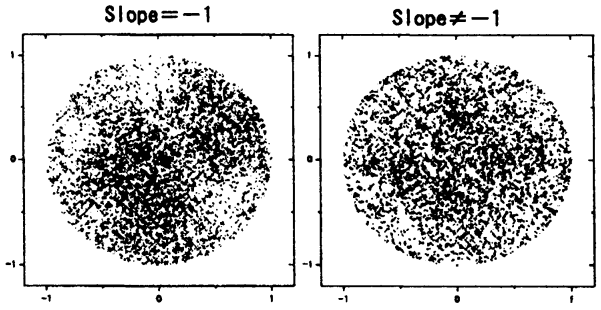

Figure 13: Equilibrium distributions of the two cases where the slope is equal to -1 and unequal to -1 are shown.

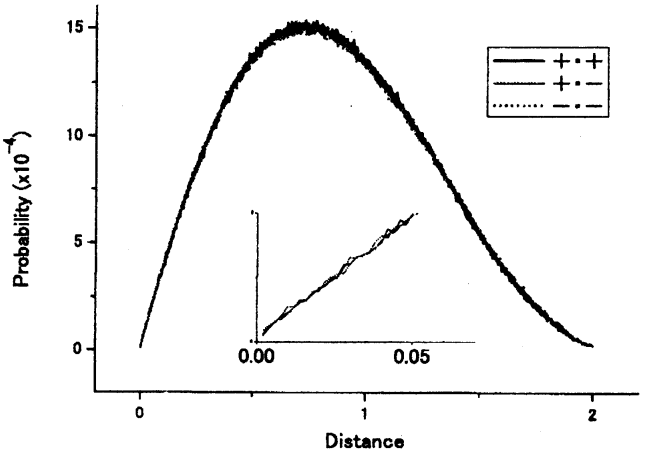

Figure 14: Two-body correlation function where the slope is equal to -1 is plotted.

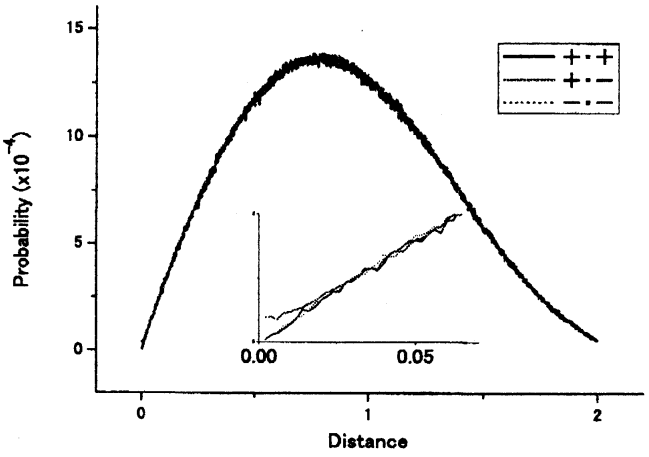

Figure 15: Two-body correlation function where the slope in unequal to -1 is plotted.

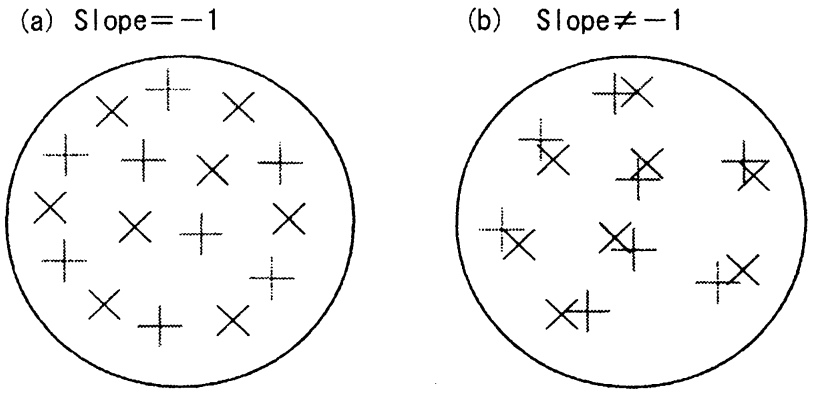

Figure 16: Two equilibrium distributions are illustrated. The signs + and × represent the positive and negative vortices, respectively.

around positive vortices and that of negative vortices around positive vortices does not match, and the cancellation of the terms in Eq. (15) is imperfect, so that the slope is not -1. The correlation functions also suggest that there are at least two equilibrium states as shown in Fig. 16.

6 Discussion

The massive numerical simulation results using the special-purpose supercomputer, MDGRAPE series have been presented to understand the statistical mechanical feature of the two-dimensional point-vortex system.

Recently, computational power has grown rapidly and PC cluster enables massive numerical simulations in university laboratory. However, simulations that can be accelerated by distributed computing is restricted, which depends mainly the physical model itself. Physical problems that need integrals over whole space, including Poisson equation, Biot-Savart integral, may be inappropriate for the distributed computing. One of the ways to solve the above problem is a special-purpose computer. Nowadays, integrated circuits that can be programmed by a user are widely used in industry, which is called Field Programmable Gate Array (FPGA). I believe the FPGA technology breaks the usability and the performance of the classic vector-type supercomputer.

I did not mention here, but an intriguing aspect of two-dimensional turbulence is a vortex crystal that is understood as a metastable state. Several ideas to understand the metastable state have been proposed. However these are applicable for only limited cases and no fundamental theory is established.

Acknowledgement

The author thanks Professor Yasuhito Kiwamoto, Professor Hiroyuki Tomita and Dr. Mitsusada M. Sano for valuable discussion. The author thanks Dr. Toshikazu Ebisuzaki, Dr. Makoto Taiji and Dr. Tetsu Narumi for a support of MDGRAPE-2 and MDGRAPE-3.

References

[1] Y. Yatsuyanagi, Y. Kiwamoto, H. Tomita, M. M. Sano, T. Yoshida, and T. Ebisuzaki. *Phys. Rev. Lett.*, Vol. 94, p. 054502, 2005.

[2] L. Onsager. *Nuovo Cimento Suppl.*, Vol. 6, p. 279, 1949.

[3] G. Joyce and D. Montgomery. *J. Plasma Phys.*, Vol. 10, p. 107, 1973.

[4] Y. B. Pointin and T. S. Lundgren. *Phys. Fluids*, Vol. 19, p. 1459, 1976.

[5] C. E. Seyler, Jr. *Phys. Fluids*, Vol. 19, p. 1336, 1976.

[6] O. Bühler. *Phys. Fluids*, Vol. 14, p. 2139, 2002.

[7] D. J. Johnson. *Phys. Fluids*, Vol. 31, p. 1856, 1988.

[8] D. H. E. Dubin and T. M. O'Neil. *Rev. Mod. Phys.*, Vol. 71, p. 87, 1999.

[9] R. C. Davidson. *Physics of nonneutral plasmas.* Imperial College, London, 2001.

[10] J. Sommeria. Two-dimensional turbulence. In M. Lesieur, A. Yaglom, and F. David, editors, *New Trends in turbulence.* Springer, 2000.

[11] P. Tabeling. *Phys. Rep.*, Vol. 362, p. 1, 2002.

[12] G. L. Eyink and K. R. Sreenivasan. *Rev.. Mod. Phys.*, Vol. 78, p. 87, 2006.

[13] D. Patterson and J. Hennessy. *Computer Organization and Design, 3rd ed.* Morgan Kaufmann, San Fransisco, 2004.

[14] T. Ito, K. Makino, T. Ebisuzaki, and D. Sugimoto. A special-purpose n-body machine grape-1. *Comput. Phys. Comm.*, Vol. 60, p. 187, 1990.

[15] T. Yoshida and M. M. Sano. *J. Phys. Soc. Jpn.*, Vol. 74, p. 587, 2005.

[16] E. A. Novikov. *Sov. Phys. JETP*, Vol. 41, p. 937, 1975.